Available online at www.sciencedirect.com

Manufacturing Letters

Manufacturing Letters 41 (2024) 907–913

52nd SME North American Manufacturing Research Conference (NAMRC 52, 2024)

Ultrasonic Vibration-assisted High-Resolution Electrohydrodynamic (EHD) Printing

Qingrui Jiang[a], Ruofan Cao[b], Yi Wang[c*], Yiwei Han[a*]

[a]*Department of Mechanical Engineering, University of Mississippi, University, MS 38677, United States*
[b]*Department of BioMolecular Sciences, University of Mississippi, University, MS 38677, United States*
[c]*Department of Industrial & System Engineering, University of Missouri, Columbia, MO 65211, United States*

* Corresponding author. Yiwei Han, Tel.: +1-662-915-3032 *E-mail address:* yhan2@olemiss.edu

Yi Wang, Tel.: +1-573-882-2340 *E-mail address:* yiwang@missouri.edu

Abstract

Electrohydrodynamic (EHD) printing has become a promising and cost-effective technique for producing high-resolution and large-scale features. One widely recognized obstacle in EHD printing is nozzle clogging due to solvent evaporation or ink polymerization. Moreover, printing highly viscous materials often requires pressure or other external force to assist the ink flow during the printing, which increases the complexity of process control and the required energy. In this work, we developed a novel ultrasonic vibration-assisted EHD printhead and associated process to effectively eliminate the nozzle clogging for the printing of high-viscosity and high-evaporation-rate inks. A series of experimental tests were conducted to characterize the printhead design and process parameters (i.e., vibration frequency, vibration amplitude, and printing voltage). The results demonstrated that superimposing ultrasonic vibration on the EHD printing nozzle can effectively enhance current EHD printing capabilities, such as reducing required pressure, eliminating nozzle clogging, and providing stable and continuous printing for high viscosity and high solvent evaporation rate material. With the optimal parameters, a filament with a diameter of around 1μm can be continuously printed. In the paper, we successfully applied this developed ultrasonic-assisted EHD process to print high-resolution 2D patterns.

Peer-review under responsibility of the Scientific Committee of the NAMRI/SME.
Keywords: Electrohydrodynamic(EHD) printing; Ultrasonic vibration; High-viscosity

1. Introduction

Electrohydrodynamic (EHD) printing is a cost-effective high-resolution printing technology that can produce fine droplets or jets with a size much smaller than the printing nozzle size [1]. In EHD printing, printing materials are subjected to a high electric field to form a Taylor-cone structure. When the electrostatic force exceeds the ink surface tension and viscose force, a fine jet or droplet will be ejected. [1]. This capability overcomes the nozzle size limitation and enables the production of parts with single-micron or sub-micron resolutions [2]. Compared with other high-resolution AM techniques (e.g., aerosol jet [3,4], electrochemical deposition-based AM [5], Two-photon photopolymerization [6–8], Micro-Selective Laser Sintering [9,10]), EHD printing doesn't require a dedicated machine or complex post-process, and it can easily accommodate various materials (e.g., such as polymers [11–13], shape memory polymers [14], conductive nano inks [15–17], quantum materials [18,19], and ceramic solutions [20,21]) for a wide range of applications. EHD printing has been proven to empower the fabrication of novel functional

Peer-review under responsibility of the Scientific Committee of the NAMRI/SME.

devices, tissue structures, and pharmaceutics [22].

While EHD printing can create features smaller than the nozzle size, it becomes more susceptible to nozzle clogging when employing smaller nozzle sizes. The issue of nozzle clogging poses a critical challenge in EHD printing due to solvent evaporation, ink drying near or within the nozzle tip, high material viscosity, and high material concentrations, which prevents utilizing EHD printing with functional and novel materials for nanoscale fabrication. For example, electrically conductive contents (e.g., particles, nanowires, flakes) are often added to a solution carrier to form functional printing inks. A high concentration of functional content suspended in the printing inks tends to aggregate or precipitate over extended periods at the nozzle tip, significantly disrupting the printing process and preventing continuous printing [23–28]. For nano-resolution EHD printing, a high-resolution nozzle with an inner diameter of a few micrometers or less is usually required [1,29–31]. The smaller nozzle diameters are more sensitive to the viscosity of the ink, increasing the risk of nozzle clogging. Extensive experiments have demonstrated that an ink viscosity of higher than 90 mPa·s will easily cause nozzle clogging, which prevents the usage of a range of polymer materials in high-resolution applications [32,33]. A dual-channel nozzle has been developed to generate a circulating ink path during EHD printing [34,35]. During the printing, ink is continuously injected into the nozzle through one flow channel and extracted from the other, thus preventing the nozzle from clogging. However, this nozzle design is unsuitable for ink with high viscosity due to the enormous withdrawing force, and it will be very challenging to fabricate a small nozzle for nanoscale printing due to the intricacies of dual-channel nozzle manufacturing. The stagnation of some materials (such as PEO, PEDOT, or PVDF) is prone to rapid drying and/or forming a thin film layer that will block the nozzle due to the low ink flow rate in EHD printing. To address this, researchers often add other solution components (e.g., ethanol, glycerin, acetone) for highly diluted inks when printing such materials [36–41]. While these adjustments may be acceptable for specific applications, they are still challenging for large-scale pattern printing, and post processes are required to remove those additives to enhance the functional performance.

Ultrasonic vibration has been demonstrated to improve various manufacturing methods for decades, including ultrasonic vibration-assisted milling [42–45], ultrasonic vibration-assisted turning [46,47], ultrasonic vibration-assisted welding [48,49], etc. Employing high-frequency vibration in manufacturing can dramatically reduce the friction force. The superimposed ultrasonic will generate a stick-slip motion between two sliding interfaces, similar to piezoelectric motors that utilize this effect [50], which can reduce the friction force. Applying ultrasonic vibration on fluid extrusion has been proven to improve the rheology (viscosity and elastic strain) and flow behavior, thus improving the extrusion process. Ultrasonic vibration was recently applied to extrusion-based 3D printing technology [51–53]. It has been found that ultrasonic vibration can improve interlayer adhesion due to decreased melt viscosity and physically modified interface wettability. Gunduz's group employs an ultrasonic actuator against the syringe nozzle to print extremely viscous materials [51]. The experiment results show that the superimposed ultrasonic vibration is able to effectively reduce wall friction and flow stresses on the nozzle, enabling a lower printing pressure requirement with precise flow control. This promising method is able to print high-viscosity materials with a smaller nozzle and increase the flow velocity of the printing materials. However, the reported ultrasonic vibration-assisted printing methods were enabled by externally attaching an ultrasonic actuator to the nozzle, limiting the study for fine-tuning the vibration characteristics. Wang et al. attach a piezoelectric actuator to a bioprinting nozzle, showing that the acoustic pressure can assist the concentration of cells/particles and improve the printing resolution [54]. Despite the superior benefits of ultrasonic vibration in 3D printing, the study of ultrasonic vibration-assisted 3D printing is still in an early stage.

To the best of our knowledge, the integration of ultrasonic vibration and EHD printing has not been explored. In this work, we have successfully designed an integrated ultrasonic vibration-assisted printhead to create a nozzle-clogging-free EHD printing of materials with high viscosity and high solvent evaporation rate. Design and process parameters have been characterized to demonstrate the effectiveness of the designed ultrasonic vibration printhead and the relationships between design and process parameters and printed filament have been studied. High-resolution grid patterns with various pitch have been printed. This work has demonstrated the potential of applying this ultrasonic vibration-assisted EHD printing process to produce high-resolution large-scale patterns for high-viscosity and high-volatile functional materials.

2. Materials and Methods

2.1. Ultrasonic vibration-assisted printhead design

A universal ultrasonic vibration-assisted printhead was designed and developed, as shown in Fig. 1, which can be easily integrated into the EHD printer or other nozzle-based printers without any interference with the current configuration. A Langevin-type ultrasonic transducer structure, consisting of 4 pieces of PZT-8 piezoceramic discs sandwiched between a back mass nut and flange, was developed to efficiently generate high-power ultrasonic vibration. A flange structure of the transducer was designed and optimized to provide stable mechanical support and efficient vibration transfer. When excited by a sinusoidal signal, the piezoceramic stack transmits a longitudinal vibration forward to the printing nozzle. In order to successfully dispense the inks, a through hole was drilled at the center of the ultrasonic transducer, and a silicone tube was embedded and connected to the upper syringe and lower Luer connectors. The designed printhead has a resonance frequency of 55 kHz. The complete setup of the printhead is shown in Fig. 1(a), consisting of components such as printhead shell, syringe, Luer adapters, and fixtures. Fig. 1(b)

is the fabricated vibration-assisted printhead used in the EHD printing experiment.

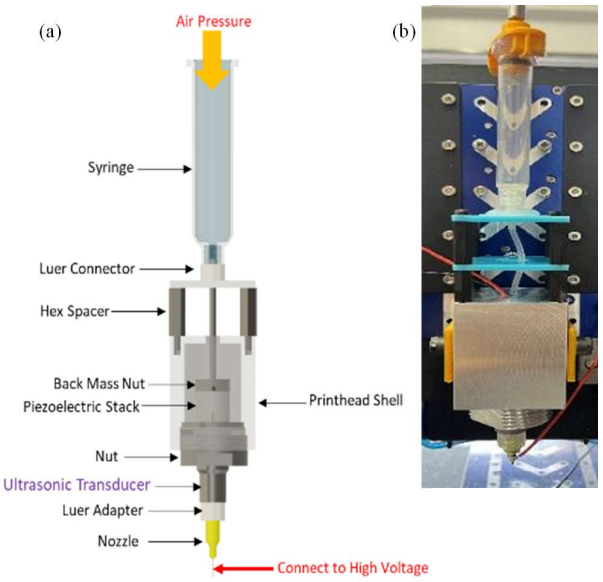

Fig. 1. (a) Illustration of the ultrasonic vibration-assisted printhead for EHD printing. (b) The fabricated vibration-assisted printhead for EHD printing in this project.

2.2. Materials and printing system

To evaluate the enhanced printing capability, high viscosity, and high evaporation rate PEO ink was selected in this paper. The printing material was prepared by mixing DI water and Poly(ethylene oxide) (PEO) powder with a molecular weight of 1,000,000. The prepared ink contained a PEO weight ratio of 4% , which has a viscosity of around 10,000 mPa·s. The ultrasonic vibration-assisted EHD printing system consisted of an ultrasonic vibration-assisted printhead, a high-precision three-axis stage with repeatability of 50 nm, a voltage supply, a pneumatic dispensing system (including a compressor and a precision regulator), and a high-resolution camera. The ultrasonic vibration printhead was connected to an ultrasonic driver (PDU210), which can control the vibration frequency and amplitude. The power of the vibration amplitude was controlled by voltage. The pressure was connected with a syringe to help the ink flow to the nozzle before printing. The high-voltage supply with a maximum voltage of 10 kV was connected to the EHD printing nozzle to generate the electrostatic force for the printing. A nozzle with an orifice of 51 µm was selected for printing. A ground electrode was placed on the motion stage, and a glass substrate was placed on the ground electrode for the EHD printing. The EHD printer was located on an optical table to reduce environmental vibration. The camera with a resolution of 1 µm was used to monitor the printing process.

2.3. Characterization of ultrasonic vibration-assisted EHD printing

2.3.1. Testing of ultrasonic vibration printhead

The PEO solution was loaded into the syringe, and a pressure of 0.4 psi was applied to the syringe to bring ink to the nozzle tip. Then, the pressure was removed from the syringe. No pressure was applied during the experiment. The vibration frequency and power of the printhead were set to 55 kHz and 75 V, respectively. The printing voltage was selected as 1 kV. To test the effectiveness of designed ultrasonic vibration-assisted printhead, three different experiments were performed. At the time of 0 seconds, both printing voltage and vibration were applied for all three experiments to avoid clogging the nozzle. For the first experiment, both printing voltage and vibration were kept after time 0; and for the second and third experiments, only printing voltage or vibration were applied in the system after time 0. A camera was used to record the printing behaviors for all three experiments.

2.3.2. Characterization of key parameters in ultrasonic vibration-assisted EHD printing

Vibration frequency, vibration amplitude, and printing voltage have been identified as key factors in ultrasonic vibration-assisted EHD printing. The ultrasonic vibration was controlled by an ultrasonic driver that can provide a vibration frequency between 20 kHz and 100 kHz and an amplitude voltage between 0 V and 105 V. Higher voltage will generate a larger amplitude, which shows a linear relationship [55]. We characterized each factor at a time with the control variable method, as shown in Table 1. The selected ranges for each factor are 35 kHz to 80 kHz for vibration frequency, 35 V to 105 V for vibration amplitude, and 0.7kV to 1.5kV for printing voltage. The standoff distance of 700 µm was selected to reduce the disturbance during the printing. The printing speed of 20 mm/s was selected to best match the EHD jetting speed. The printed filaments were observed and measured using Zeiss Axio Imager M1 with the pre-installed measuring software. The software can automatically change the scaling based on the selected lens, and it can directly provide measuring data between two points.

Table 1. The overview of tested parameter.

Experiment	Frequency / Hz	Vibration Power / V	Voltage / kV
Frequency study	35000-80000	75	1
Amplitude study	55000	35-105	1
Voltage study	55000	75	0.7-1.5

2.4. High-resolution 2D printing

The optimal vibration and printing parameters identified in the characterization process were used for patterning. A grid pattern was meticulously designed in the ACS SPC software and directly transferred to SPiiPlus MMI for direct printing. The printing speed was 20 mm/s to provide the best printing performance. Grid patterns with two different pitches (i.e., 20 µm, and 100 µm) were used to demonstrate

the production capability of the developed EHD printing process. The printed patterns were observed and measured using an optical microscope.

3. Results and Discussion

3.1. Characterization results for ultrasonic vibration-assisted EHD printing

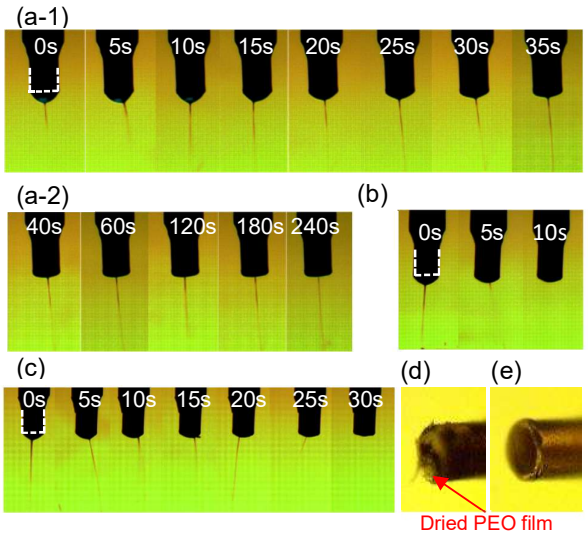

Fig. 2. Optical images of printing behaviours at different time (seconds) under different printing conditions. White dash-line outlines the nozzle. (a1-2) Printing with both voltage and ultrasonic vibration. (b) Printing with vibration only. (c) Printing with voltage only. (d) The clogged nozzle after 30s of printing with high vlotage only. (e) The unused nozzle before printing.

The effectiveness of the designed ultrasonic vibration printhead is first tested. Fig. 2 shows the printing behavior under three different printing conditions. At time 0, a fine jet can be observed for all three conditions. Fig. 2 (a-c) with a time of 0 shows the printing behavior when both vibration and printing voltage were applied to the system. Initially, a Taylor cone was formed at the nozzle tip, and a fine jet was produced. The cone was evolving during the first 35 seconds, and a stable cone shape formed after 35 seconds (Fig. 2 (a-1)). This cone shape allowed continuous stable jetting for over 3 minutes in the experiment, demonstrating the long-period printing capability (Fig. 2 (a-2)). Fig. 2 (b) shows the printing behavior when only vibration is applied. In the absence of an electric field, it lacks sufficient force to carry out the ink. As a result, the cone contracted, and no inkjet was observed even after a 10-second. Fig. 2 (c) shows the printing behavior when only voltage is applied. At the beginning (from 0 to 20 seconds), a jet can be formed. However, the shape of the cone continues to change, and an unstable jetting behavior can be observed. At the time of 25 seconds, the cone contracted, and only a small amount of materials was carried out from the nozzle, which indicated the drying process of the PEO material. When the drying rate or the solution evaporation rate is higher than the material jetting rate, a dried film starts to form at the nozzle tip. The film will expand from the edge to the center and eventually cover all areas of the nozzle tip, resulting in nozzle clogging. Fig. 2 (d-e) shows a clogged nozzle after printing without applying vibration compared to a brand-new nozzle. Moreover, during the material drying process, the cone dynamically changes, thus resulting in an unstable printing starting from the initial stage. This unstable printing process indicated that only applying voltage is not enough for even a short period of printing. All of these results demonstrated that superimposing ultrasonic vibration can effectively prevent the ink from drying and help to provide a stable fine jetting process. The mechanism can be explained as introducing the vibration to the printing system, which can reduce the ink shear stress and friction between the ink and nozzle walls, thus increasing the ink flow rate in the nozzle. When the ink flow rate is higher than the evaporation rate or material drying rate, continuous jetting can be obtained.

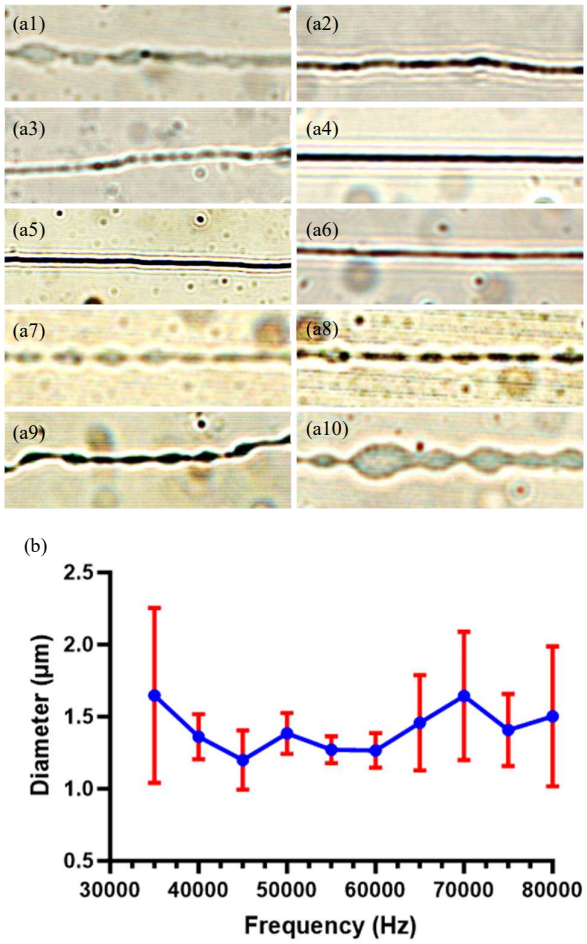

Fig. 3. (a1-a10) The optical images of printed filaments with different vibration frequencies from 35 kHz to 80 kHz. (b) The relationship between the applied vibration frequency and filament diameter.

Vibration frequency, vibration amplitude, and applied printing voltage are the key factors affecting the printing behavior and results. Fig. 3 shows the printed filament under different vibration frequencies. There are no obvious changes in the filament diameters, but the quality of the filament varies among different frequencies. Based on the design, the printhead used in this experiment has a resonance frequency of 55 kHz. When the vibration frequency was close to this frequency, more uniform filaments can be obtained, as shown in Fig. 3 (a4-a6). When the vibration

frequency deviated from the resonance frequency, filaments with irregular shapes were observed in Fig. 3 (a1-a3 and a7-a10). This can be explained as that when the vibration frequency is close to the resonance frequency, the tip of the printhead can reach the maximum amplitude, which can significantly reduce the ink viscosity, thus increasing the ink flow rate and reducing the required force to carry out the ink.

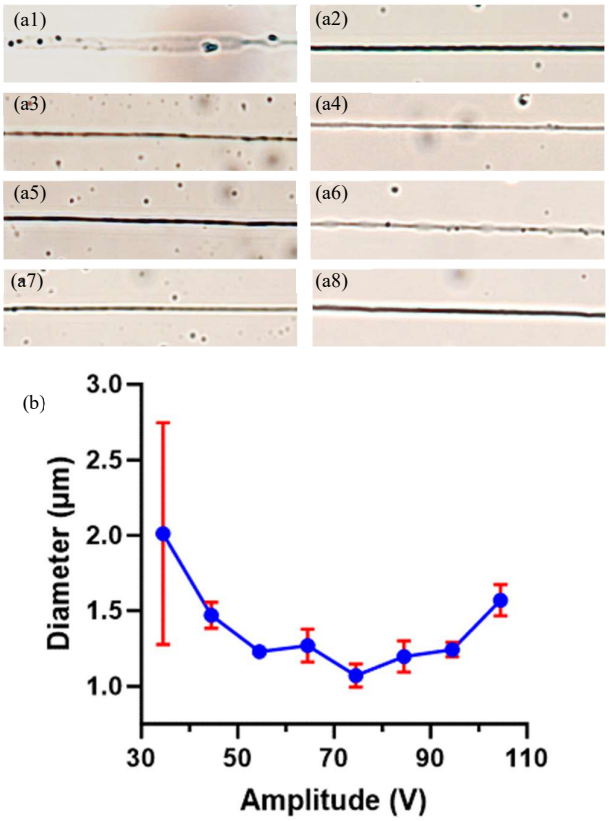

Fig. 4. (a1-a8) The optical images of printed filaments with different amplitude voltages from 35V to 105V. (b) The relationship between the applied amplitude and filament diameter.

Fig. 4 shows the relation between the vibration amplitude and filament diameter with a vibration frequency of 55 kHz and an applied voltage of 1 kV. When a small amplitude voltage of 25 V was applied, filaments with large variances in diameter were printed, which is shown in Fig. 4 (a1). The small vibration amplitude will only reduce little ink shear stress; thus, it still requires a larger force to carry out the ink. When the applied printing voltage cannot provide enough force, irregular filaments are printed. When gradually increasing the amplitude power to 75 V, a more uniform filament can be observed, and the diameter of the filament decreased (Fig. 4 (a2-a5)). Moreover, less variation was seen in those filament dimensions, indicating the stable printing process. This can be explained by the fact that increasing the voltage will increase the amplitude, thus further reducing the ink shear stress and the required force for continuous printing. After continuously increasing the amplitude voltage, the filament diameter also increased (Fig. 4 (a6-a8)). A higher vibration amplitude will dramatically reduce the ink viscosity, and ink will easily be swung out due to the large vibration amplitude, resulting in an increased diameter.

Fig. 5 describes the relationship between the applied printing voltage and filament diameter when applying a constant vibration frequency of 55 kHz and amplitude power of 75 V. When the printing voltage was less than 0.7 kV, no filament was printed on the substrate. After applying a voltage of 0.7 kV, a filament can be observed in Fig. 5 (a1). However, due to the insufficiency of the voltage, the printed

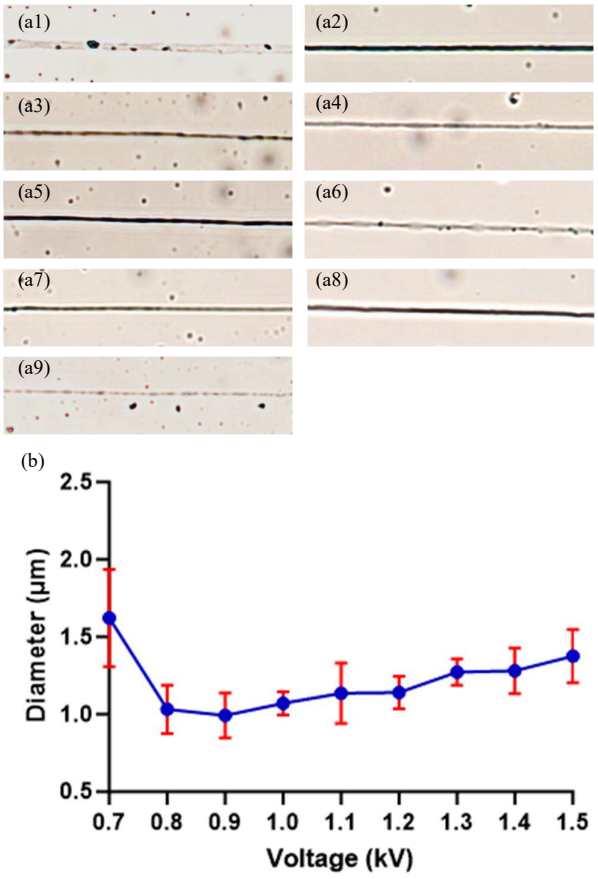

Fig. 5. (a1-a9) The optical images of printed filaments with different printing voltage from 0.7kV to 1.5kV. (b) The relationship between the applied voltage and filament diameter.

filament exhibited an ununiform shape and large variation in diameter. When applying a voltage of 0.8kV, a continuous straight filament is ejected from the Taylor-cone, indicating a stable jetting shown in Fig. 5 (a2). Further increasing the voltages, the diameters were increased, as shown in Fig. 5 (a3-a9). Increasing the voltage will increase the electrostatic force; thus, more materials can be carried out. With the same printing speed, a larger diameter will be obtained to match the ejected volume of materials.

Optimal process parameters were obtained from the previous experiments. Filament with the smallest diameter and less variance in diameter is the best for high-resolution patterning. To achieve the best printing result, the vibration frequency, amplitude power voltage, and applied printing voltage were selected as 55 kHz, 75 V, and 1 kV. Fig. 6 shows the printed 2D patterns. With the selected process parameters, filaments with a diameter of around 1 μm, which is about 1/50 of the nozzle orifice, can be printed during the printing process. Fig. 6 (a) shows a grid with a pitch of 20

μm can be successfully printed. Fig. 6 (b) shows the printed grid on the substrate when the sample was positioned between the camera and the light source. Two grids can be barely found on the substrate, which are pointed by the two arrows. However, when placing the sample on another surface that isn't directly exposed to the light, the printed grids showed great optical transparency (Fig. 6(c)). The two grids are almost invisible to the human eyes. Fig. 6 (d) - (f) shows printed two 5mm x 8mm large-scale patterns with a pitch of 100 μm. The results show that fine grids can be printed even with high printing speed for large-scale patterns. Moreover, the printed grids show excellent transparency. When placing the printed grids on a colored surface, they are invisible to the human eyes (Fig. 6 (g)). Compared with the grids exposed under the light (Fig. 6 (f)), no grid can be observed in Fig. 6 (g). All results demonstrated the excellent

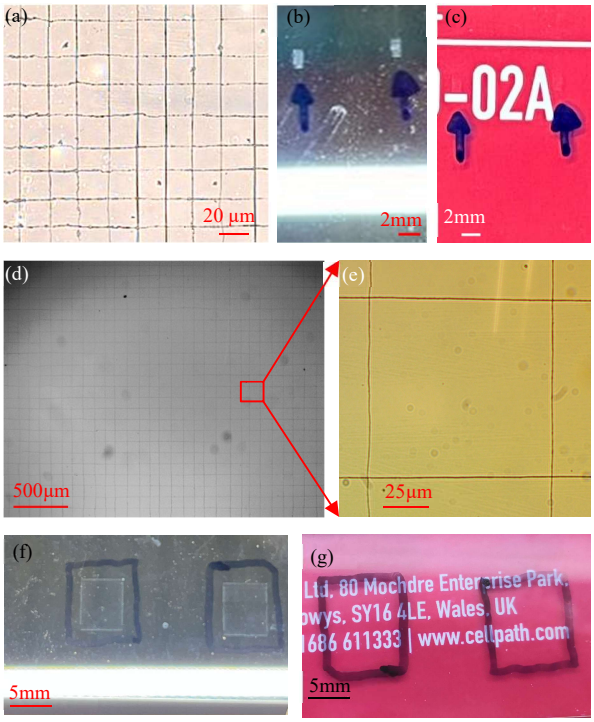

Fig. 6. (a) Printed grid with a pitch of 20 μm. (b) Optical image when placing the sample between camera and light source. (c) Optical image when placing the sample on a substrate. (d) Printed grid with a pitch of 100 μm. (e) Microscope image of a small area of a printed grid with a 100 μm gap. (f) Optical image when placing the sample between the camera and light source. (g) Optical image when placing the sample on the substrate.

stability of the developed ultrasonic vibration-assisted EHD printing process for large-scale high-resolution patterning as well as the potential of applying this novel printing process for fabricating transparent patterns.

4. Conclusions

In this work, we successfully designed and developed an ultrasonic vibration-assisted EHD printhead to achieve a nozzle-clogging free printing of high viscosity and high solvent evaporation rate materials. Design and process parameters have been characterized to demonstrate the effectiveness of the developed printhead and study the relationship between process parameters and printing characteristics. High-resolution grid patterns with different pitches have been printed. This work has demonstrated the potential of applying this ultrasonic vibration-assisted EHD printing process to produce high-resolution patterns for high viscosity and highly volatile functional materials in a cost-effective manner. The result also provides a promising potential for integrating vibration with other types of printing technologies, such as inkjet printing and direct ink writing [56]. In the future, various high-viscosity materials such as slurry, conductive paste, and hydrogel, can be investigated to further explore the capability of vibration-assisted EHD printing for different applications.

Acknowledgments

This work was supported in part by a grant from the National Science Foundation (NSF) (IOS-2200200) and an Institutional Development Award (IDeA) from the National Institute of General Medical Sciences of the National Institutes of Health (NIH-P20GM103460).

5. References

[1] Park J-U, Hardy M, Kang SJ, Barton K, Adair K, Mukhopadhyay DK, et al. High-resolution electrohydrodynamic jet printing. Nat Mater 2007;6:782–9.
[2] Han Y, Dong J. Electrohydrodynamic printing for advanced micro/nanomanufacturing: Current progresses, opportunities, and challenges. J Micro Nanomanuf 2018;6. https://doi.org/10.1115/1.4041934.
[3] Secor EB. Principles of aerosol jet printing. Flex Print Electron 2018;3:035002.
[4] Wilkinson NJ, Smith MAA, Kay RW, Harris RA. A review of aerosol jet printing—a non-traditional hybrid process for micro-manufacturing. Int J Adv Manuf Technol 2019;105:4599–619.
[5] Xu J, Ren W, Lian Z, Yu P, Yu H. A review: development of the maskless localized electrochemical deposition technology. Int J Adv Manuf Technol 2020;110:1731–57.
[6] Zhou X, Hou Y, Lin J. A review on the processing accuracy of two-photon polymerization. AIP Adv 2015;5:030701.
[7] Wloka T, Gottschaldt M, Schubert US. From light to structure: Photo initiators for radical two-photon polymerization. Chemistry 2022;28:e202104191.
[8] Lee K-S, Yang D-Y, Park SH, Kim RH. Recent developments in the use of two - photon polymerization in precise 2D and 3D microfabrications. Polym Adv Technol 2006;17:72 – 82.
[9] Nagarajan B, Hu Z, Song X, Zhai W, Wei J. Development of micro selective laser melting: The state of the art and future perspectives. Engineering (Beijing) 2019;5:702–20.
[10] Fu J, Hu Z, Song X, Zhai W, Long Y, Li H, et al. Micro selective laser melting of NiTi shape memory alloy: Defects, microstructures and thermal/mechanical properties. Opt Laser Technol 2020;131:106374.
[11] Wei C, Dong J. Direct fabrication of high-resolution three-dimensional polymeric scaffolds using electrohydrodynamic hot jet plotting. J Micromech Microeng 2013;23:025017.
[12] Han Y, Wei C, Dong J. Super-resolution electrohydrodynamic (EHD) 3D printing of micro-structures using phase-change inks. Manuf Lett 2014;2:96–9.
[13] Nothnagle C, Baptist JR, Sanford J, Lee WH, Popa DO, Wijesundara MBJ. EHD printing of PEDOT: PSS inks for fabricating pressure and strain sensor arrays on flexible substrates. In: Popa D, Wijesundara MBJ, Blowers M, editors. Next-Generation Robotics II; and Machine Intelligence and Bio-inspired Computation: Theory and Applications IX, SPIE; 2015. https://doi.org/10.1117/12.2177415.
[14] Stretchable Circuits via Electric-Field-DrivenMicroscale 3D Printing for Localized Heating of Shape MemoryPolymers in 4D Printing. n.d.

[15] Cui Z, Han Y, Huang Q, Dong J, Zhu Y. Electrohydrodynamic printing of silver nanowires for flexible and stretchable electronics. Nanoscale 2018;10:6806–11.
[16] Lee D-Y, Shin Y-S, Park S-E, Yu T-U, Hwang J. Electrohydrodynamic printing of silver nanoparticles by using a focused nanocolloid jet. Appl Phys Lett 2007;90:081905.
[17] Rahman K, Khan A, Muhammad NM, Jo J, Choi K-H. Fine-resolution patterning of copper nanoparticles through electrohydrodynamic jet printing. J Micromech Microeng 2012;22:065012.
[18] Li H, Duan Y, Shao Z, Zhang G, Li H, Huang Y, et al. High‐resolution pixelated light emitting diodes based on electrohydrodynamic printing and coffee‐ring‐free quantum dot film. Adv Mater Technol 2020;5:2000401.
[19] Wang H, Zhang Y, Liu Y, Chen Z, Li Y, Li X, et al. High-efficiency and high-resolution patterned quantum dot light emitting diodes by electrohydrodynamic printing. Nanoscale Adv 2023;5:1183–9.
[20] Wang DZ, Edirisinghe MJ, Jayasinghe SN. Solid freeform fabrication of thin-walled ceramic structures using an electrohydrodynamic jet. J Am Ceram Soc 2006;89:1727–9.
[21] Lee D-Y, Yu J-H, Shin Y-S, Park D, Yu T-U, Hwang J. Formation of ceramic nanoparticle patterns using electrohydrodynamic jet printing with pin-to-pin electrodes. Jpn J Appl Phys (2008) 2008;47:1723–5.
[22] Onses MS, Sutanto E, Ferreira PM, Alleyne AG, Rogers JA. Mechanisms, capabilities, and applications of high-resolution electrohydrodynamic jet printing. Small 2015;11:4237–66.
[23] Calvert P. Inkjet Printing for Materials and Devices. Chem Mater 2001;13:3299–305.
[24] Molesa S, Redinger DR, Huang DC, Subramanian V. High-quality inkjet-printed multilevel interconnects and inductive components on plastic for ultra-low-cost RFID applications. Mater Res Soc Symp Proc 2003;769. https://doi.org/10.1557/proc-769-h8.3.
[25] Hoth CN, Choulis SA, Schilinsky P, Brabec CJ. High photovoltaic performance of inkjet printed polymer:Fullerene blends. Adv Mater 2007;19:3973–8.
[26] Nallan HC, Sadie JA, Kitsomboonloha R, Volkman SK, Subramanian V. Systematic design of jettable nanoparticle-based inkjet inks: rheology, acoustics, and jettability. Langmuir 2014;30:13470–7.
[27] Chen S-P, Chiu H-L, Wang P-H, Liao Y-C. Inkjet printed conductive tracks for printed electronics. ECS J Solid State Sci Technol 2015;4:P3026–33.
[28] Kwon J, Hong S, Suh YD, Yeo J, So H-M, Chang WS, et al. Direct micro metal patterning on plastic substrates by electrohydrodynamic jet printing for flexible electronic applications. ECS J Solid State Sci Technol 2015;4:P3052–6.
[29] Zou W, Yu H, Zhou P, Liu L. Tip-assisted electrohydrodynamic jet printing for high-resolution microdroplet deposition. Mater Des 2019;166:107609.
[30] Miskovic G, Kaufhold R. Additive manufacturing for nano-feature applications: Electrohydrodynamic printing as a next-generation enabling technology. IEEE Open J Nanotechnol 2022;3:191–8.
[31] Qin H, Dong J, Lee Y-S. AC-pulse modulated electrohydrodynamic jet printing and electroless copper deposition for conductive microscale patterning on flexible insulating substrates. Robot Comput Integr Manuf 2017;43:179–87.
[32] Su S, Liang J, Wang Z, Xin W, Li X, Wang D. Microtip focused electrohydrodynamic jet printing with nanoscale resolution. Nanoscale 2020;12:24450–62.
[33] Easy Printing of High Viscous Microdots by Spontaneous Breakup of Thin Fibres. n.d.
[34] Li Z, Al-Milaji KN, Zhao H, Chen D-R. Ink bridge control in the electrohydrodynamic printing with a coaxial nozzle. J Manuf Process 2020;60:418–25.
[35] Li Z, Al-Milaji KN, Zhao H, Chen D-R. Electrohydrodynamic (EHD) jet printing with a circulating dual-channel nozzle. J Micromech Microeng 2019;29:035013.
[36] Lee H, Seong B, Kim J, Jang Y, Byun D. Direct alignment and patterning of silver nanowires by electrohydrodynamic jet printing. Small 2014;10:3918–22.
[37] Zhang B, Li S, Qureshi MSH, Mia U, Ge Z, Song A. In-situ assembly of MoS2 nanostructures on EHD-printed microscale PVDF fibrous films for potential energy storage applications. Polymers (Basel) 2022;14:5250.
[38] Yu M, Ahn KH, Lee SJ. Design optimization of ink in electrohydrodynamic jet printing: Effect of viscoelasticity on the formation of Taylor cone jet. Mater Des 2016;89:109–15.
[39] Li W, Wang X, Zheng G, Xu L, Jiang J, Luo Z, et al. Current characteristics of stable cone–jet in electrohydrodynamic printing process. Appl Phys A Mater Sci Process 2018;124. https://doi.org/10.1007/s00339-018-2133-0.
[40] Rivers G, Austin JS, He Y, Thompson A, Gilani N, Roberts N, et al. Stable large area drop-on-demand deposition of a conductive polymer ink for 3D-printed electronics, enabled by bio-renewable co-solvents. Addit Manuf 2023;66:103452.
[41] Jain K, Wang Z, Garma LD, Engel E, Ciftci GC, Fager C, et al. 3D printable composites of modified cellulose fibers and conductive polymers and their use in wearable electronics. Appl Mater Today 2023;30:101703.
[42] Ni C, Zhu L, Liu C, Yang Z. Analytical modeling of tool-workpiece contact rate and experimental study in ultrasonic vibration-assisted milling of Ti–6Al–4V. Int J Mech Sci 2018;142–143:97–111.
[43] Chen W, Huo D, Shi Y, Hale JM. State-of-the-art review on vibration-assisted milling: principle, system design, and application. Int J Adv Manuf Technol 2018;97:2033–49.
[44] Ni H, Wang Y, Gong H, Pan L, Li ZJ, Wang D. A novel free-form transducer for the ultra-precision diamond cutting of die steel. Int J Adv Manuf Technol 2018;95:2185–92.
[45] Wang Y, Gong H, Fang FZ, Ni H. Kinematic view of the cutting mechanism of rotary ultrasonic machining by using spiral cutting tools. Int J Adv Manuf Technol 2016;83:461–74.
[46] Yang Z, Zhu L, Zhang G, Ni C, Lin B. Review of ultrasonic vibration-assisted machining in advanced materials. Int J Mach Tools Manuf 2020;156:103594.
[47] Mohapatra S, Panda A, Kumar R, Kumar Sahoo A. Recent trends and future perspectives on vibration assisted turning: A brief review. IOP Conf Ser Mater Sci Eng 2019;653:012037.
[48] Muhammad NA, Wu CS. Ultrasonic vibration assisted friction stir welding of aluminium alloy and pure copper. J Manuf Process 2019;39:114–27.
[49] Chinchanikar SS, Gaikwad VS. State of the art in friction stir welding and ultrasonic vibration-assisted friction stir welding of similar/dissimilar aluminum alloys. Journal of Computational & 2021.
[50] Uchino K. Piezoelectric ultrasonic motors: overview. Smart Mater Struct 1998;7:273–85.
[51] Fleck TJ, McCaw JCS, Son SF, Gunduz IE, Rhoads JF. Characterizing the vibration-assisted printing of high viscosity clay material. Addit Manuf 2021;47:102256.
[52] McCaw JCS, Fleck TJ, Tejada-Ortigoza V, Patel B, Son SF, Gunduz IE, et al. Vibration-assisted printing of highly viscous food. Addit Manuf 2022;56:102851.
[53] Afriat A, Bach JS, Gunduz I, Rhoads JF, Son SF. Comparing the capabilities of vibration-assisted printing (VAP) and direct-write additive manufacturing techniques. Int J Adv Manuf Technol 2022;121:8231–41.
[54] Shao MH, Cui B, Zheng TF, Wang CH. Ultrasonic-assisted 3D bioprinting a composite of alginate and particles/cells. J Phys Conf Ser 2021;1798:012016.
[55] Wang Y, Cai Y, Gong H, Lee Y-S. Design and 3D printing of waveguide-based ultrasonic longitudinal-torsional transducers for medical needle insertion. Sens Actuators A Phys 2022;344:113706.
[56] Tran V-T, Wei Y, Du H. Influence of thermal treatment on electronic properties of inkjet-printed zinc oxide semiconductor. Int J Smart Nano Mater 2022;13:330–45.